

Air-entrained Concrete: Relationship between Thermal Conductivity and Pore Distribution Analyzed by X-Ray Tomography

A. P. Peruzzi¹, J. A. Rossignolo² and H. Kahn³

1. Faculty of Civil Engineering, Universidade Federal de Uberlândia, Minas Gerais 38400-902, Brazil

2. Faculty of Science and Food Engineering of Pirassununga, USP, São Paulo 13635-900, Brazil

3. Department of Mining and Petroleum Engineering, Polytechnic School, USP, São Paulo 05508-010, Brazil

Abstract: The thermal conductivity values of ordinary concrete can be adjusted to those prescribed in constructions by entraining air bubbles to reduce the density of concrete in order to achieve good thermal insulation. This paper concerns the analysis of air bubble distribution in concrete obtained by micro X-ray μ CT (computed tomography) and correlates it with its thermal conductivity (k). The samples were prepared of ordinary concrete varying the density by air-entraining additives, ranging between 2,277 kg/m³ and 1,779 kg/m³, aiming to correlate the mechanical properties and k with the characteristics of the bubble distribution. The results show that air-entrainment leads to viable use of this material as sealer to achieve good thermal insulation, and it can be adjusted, but there seems to be a limit to air entraining. By analysis of the μ CT images, it was possible to correlate the more quantity of bubbles of smaller diameter with the minor k , in dry or wet state, and to prove that there is a limit in the entrapped air content, and if it is exceeded, the coalescence occurs.

Key words: Concrete, pore size distribution, thermal analysis, microstructure, image analysis.

1. Introduction

Many factors have to be taken into account during the project design of a building, parameters such as the sun orientation and wind predominance, position and size of the doors and windows, shading, etc., but the thermal characteristics of the building envelope largely influence the thermal and energy performance of buildings [1]. Thus, in addition to the mechanical parameters (compressive strength, Young's modulus, density, etc.), one should also consider the water vapor absorption, transmission and Thermal conductivity (k), etc.

The use of "cast-in-situ reinforced concrete walls" as exterior sealer represents an economical and quick alternative to masonry or panel systems due to its versatility. However, ordinary concrete has high k ,

value that represents disadvantage if compared to materials considered as of good thermal performance. On average, the k on conventional concrete (at room temperature) ranges between 1.4 W/m.K and 3.6 W/m.K [2, 3], in that case the use of concrete in walls requires adjusting its thermal performance to the one required in buildings and is possible to make the properties of concrete meet the construction requirement by varying material parameters such as cement past composition, foam size and volume fraction [4]. A k about 0.8 W/m.K can be considered appropriate to use on concrete utilized in walls as sealing.

In concrete, as it occurs with the other porous construction materials, heat transfer is dominated by thermal conduction [4] and it happens by two ways: by conduction through the solid phase of concrete, usually called "skeleton", composed of aggregate and cement paste, or by flow (water or air) through the voids of

Corresponding author: A. P. Peruzzi, PhD, associate professor; research fields: construction materials, and construction systems.

concretes [5]. Thus, the density of concrete can be decreased by using light aggregates or air-entrained concrete (as in this work) in which air-bubbles are entrapped in the mortar matrix by means of a suitable aerating agent. Air-entrained concrete can be classified as NAAC (non-autoclaved aerated concrete) or AAC (autoclaved aerated concrete) based on the curing method. While the AAC is fabricated from the aluminum powder and cement (or lime) reaction (forming H_2 bubble), with added sand and water by autoclave process of curing, NAAC is made from an ordinary concrete to which bubbles of air are entrained by adding air-entraining additive (E_{air}) [6].

The good thermal insulation is more evident in the AAC that has a density ranging between 500 kg/m^3 and $1,000 \text{ kg/m}^3$, but it is difficult to fulfill the structural function for this material due to the limitations imposed by its low mechanical resistance. Using air-entraining methods in ordinary concrete (NAAC), as was the object of this work, it is possible to obtain density values ranging between $1,800 \text{ kg/m}^3$ and $2,200 \text{ kg/m}^3$ and, consequently, lower k values and, in addition, get a structural concrete produced cast-in-situ because the appropriate relationship between "air-entrained" and "mechanical parameters required" can be controlled during concrete manufacturing [6]. Regarding compressive strength (f_c) and the bulk density (γ) of concrete the EF (efficiency factor) has been used to classify a structural lightweight concrete, as Eq. (1):

$$EF = f_c / \gamma \text{ (MPa.dm}^3\text{/kg)} \quad (1)$$

In this paper, mechanical properties and thermal performance are correlated through the value EF and k .

Concerning the empty spaces in ordinary concrete, some air is always introduced during its mixing and transport, and normally taken out at the vibration. The "capillary pores" are those originated from the evaporation of water and, it represents risks to the durability of the reinforced concrete due to their connectivity. A higher empty space volume leads to lower density and k , but this can put the durability of

structural concrete at risk if the bubbles are large or connected. On the other hand, purposely entrained air bubbles (as in NAAC) are spherical, stable, elastic and have a typical distribution with diameters ranging from $10 \mu\text{m}$ to $500 \mu\text{m}$ [7], and supposedly are not connected. Regarding the concrete used in cast-in-situ reinforced walls, it has greater fluidity and the air bubbles can move more freely, enabling their coalescence and/or rupturing [8] making their connection possible and denoting risks to the durability. Foamed concrete with higher air content tends to result in larger and connected air bubbles because there is not enough mass to prevent the air voids from coalescing [4]. Therefore, a greater number of small bubbles, unconnected, represent an effective way to decrease concrete density and k without compromising durability. Smaller pores have substantial influence in governing k , for example, the increase of bubbles with diameter around $50 \mu\text{m}$ leads to a reduction in Thermal conductivity. Also the correlation between thermal performance [9] and diameter creates better results when the later is $50 \mu\text{m}$ instead of $90 \mu\text{m}$. This paper aims to quantify the number of bubbles, their diameter and volume (bubbles smaller than $500 \mu\text{m}$ are considered "purposely entrapped air" while the bigger ones are considered "occasionally entrapped air" or "from coalescence" of smaller bubbles), seeking the correlation how a greater amount of small bubbles influences the decrease of the k value of concrete under different moisture conditions.

To determine the quantity and the characteristics of the entrained air bubbles in hardened concrete, the literature mentions several methods: SEM (scanning electron microscopy), MIP (mercury intrusion porosimetry), automatic image analysis (by special video camera system and computing/digitizing techniques) and gas permeability [6]; stereoscopic microscope (EN 480-11) and CT (computed tomography) [9]. Hilal, Thom and Dowson [10] made an interesting study on pore size distribution of foamed concrete by optical microscope treating the foam with

bitumen emulsion and could see by clear image the bubbles merged and its shape and distribution.

In this research, for the microstructural analysis, micro X-ray computed tomography (μ CT) was the chosen method because it provides a reconstruction of the exact three-dimensional (3D) position of all objects of interest, and derive air bubbles parameters not available to traditional 2D test methods [11] with a quality close to real. This method has an advantage over conventional microstructural analysis methods (e.g. optical microscope, SEM) which normally require fracturing or polishing of samples, changing the internal structure. We highlight that, in this study, the samples were prepared specially for the analysis by μ CT instead of extracted by cutting them from a larger sample, and thus there was no change in the original structure of the bubbles. We have studied images obtained by μ CT to establish how the diameter distribution and quantity of the air bubbles influence the value of the thermal conductivity in concretes with different bulk density (γ) obtained by the use of air entraining additives (E_{air}) and under different moisture contents.

The moisture content was important to study because, in addition to temperature, the thermal conductivity is influenced by the percentage of moisture present in the pores of the material, increasing as moisture content increases [12]. The concrete samples were obtained by varying the mixing time to control the amount of entrained air, and this procedure was performed because the mixing characteristics have a dominant influence on the density, distribution, shape

and size of the air bubbles created [13].

2. Experimental Procedure

2.1 Materials and Methods

An ordinary concrete mix, called REF (reference), was prepared with OPC (ordinary Portland cement) conforming to the Type III (ASTM C150), sand (maximum diameter 2.4 mm and fineness modulus 2.15), crushed stone (12.7 mm or 1/2 in.), water to w/c = 0.43 and 1.0% (by cement weight) of plasticizing additive (Table 1).

The placement of the material that forms REF concrete was: 1st—80% of the amount of water; 2nd—crushed stone; 3rd—OPC; 4th—plasticizing additive; 5th—20% of the water remaining; and finally the sand content.

From the “Reference” concrete it was made the NAAC by the addition of air-entraining additive (E_{air}) with 0.25% of cement weight and mixed in the mixer for 1, 3 and 4 minutes, resulting in the concrete samples “NAAC1”, “NAAC3” and “NAAC4”, respectively.

For each type of sample cylindrical specimens (diameter = 50 mm and height = 100 mm) were prepared as recommended by ASTM C34-13 [14]. Next, they were kept in a wet room for seven days before determining their compressive strength, density, absorption (%), and structural empty spaces (%) as recommended by ASTM C642-13 [15].

For microstructural analysis in micro X-ray computed tomography cylindrical specimens (diameter = 19 mm and height = 40 mm) were molded from each type of concrete, but taking off the particles

Table 1 Summary of the mixture proportions of concrete REF.

Constituents	Mass (kg/m ³)
OPC	492
Sand	739
Crushed stone	985
Plasticizing additive	4.9
Air-entraining additive (E_{air})	0
Water	206.7

bigger than 4.8 mm, they were casted and conserved in a wet room for seven days. When these cylindrical specimens were prepared, the larger stones of the concrete were discarded to be compatible with the diameter of the mold (19 mm). Next, the samples were dried at 105 °C until reaching constant weight.

From the 3D images obtained by μ CT the bubbles distribution was quantified in the following diameter groups 0-50 μ m; 50-100 μ m; 100-150 μ m; 150-200 μ m; 200-250 μ m; 250-300 μ m; 300-350 μ m; 350-400 μ m; 400-450 μ m; 450-500 μ m and >500 μ m. Fig. 1 shows the 3D image from μ CT Xradia 510 Versa (sample REF), to exemplify, segmenting the bubbles in different colors according to their diameters using the AVIZO 8.0 software.

The thermal conductivity k was determined by ASTM E1530-11 using cylindrical specimens with

diameter (D) = 50 mm and height (h) = 25 mm (Fig. 2), obtained from the cutting of cylindrical samples with D = 50 mm and h = 100 mm, and the temperature in the steady state was 30 °C [16].

In this work, the k values of the samples were tested in the “moist state” after being exposed in a wet room for three different times (24 h, 48 h and 96 h) and determined by Eq. (2), with moisture ranging between 0% and 6% and in the “dry state”.

$$\text{Moisture contents} = [(m_m - m_d) / m_d] \times 100 \quad (2)$$

Where, m_m is mass of surface-dry sample in air after exposed in wet room and m_d is mass of oven-dried sample at 100 °C in drying oven.

The temperature of the sample material affects the k value [17], so to eliminate this influence k was determined on samples at ambient temperature (\approx 25 °C). To correlate the thermal conductivity of the

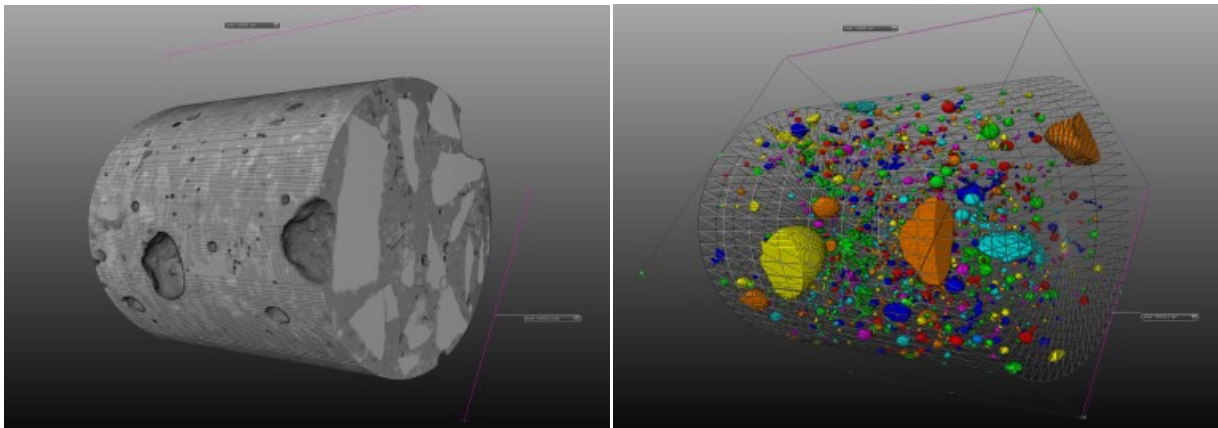


Fig. 1 Example of 3D image captured by the μ CT and distribution of false color bubbles according to their diameters.



Fig. 2 Samples 50 mm diameter and 25 mm of height obtained from the cylindrical samples (D = 50 mm and h = 25 mm) for the Thermal conductivity analyses.

samples and their microstructural view, samples REF, NAAC3 and NAAC4 were used.

2.2 Statistical Analysis

To analyze the statistical validity of the results the Chauvenet criterion was used.

3. Results and Discussion

3.1 Mechanical Properties of Hardened Concrete

Table 2 shows the mechanical properties of the specimens and verifies that compressive strength and EF decrease while the density decreases, as expect, but regarding the properties “absorption after immersion” and “% of voids” for NAAC4 samples, it shows a different trend, and both of these are smaller than for NAAC3, while the compressive strength and γ follow the logic in the series.

3.2 Thermal Conductivity of Hardened Concrete at Different Moisture Contents

Table 3 shows the k results for the concrete samples after being exposed to a wet room and withdrawal in three different times: after 24 h, 48 h and 56 h. For each sample was determined the moisture contents by Eq. (2) and the results were grouped in three different ranges: 0%-2%; 2%-4% and 4%-6%.

NAAC1, NAAC3 and NAAC4 have almost the same

thermal conductivity (0.72 W/m.K and $k = 0.71$ W/m.K, respectively) in dry state, but when the moisture of samples ranges between 4% and 6%, k values vary increasing 33% to NAAC1, 30% to NAAC3 and 59% to NAAC4. These values of k to several type of concrete studied (including in wet state) are compatible with the materials known to have good thermal performance, such as ceramic bricks (0.7 W/m.K and 1.05 W/m.K).

Fig. 3 illustrates how k varies with moisture content and a linear relationship between k and the moisture content can be observed.

Table 3 shows that NAAC1 and NAAC3 have a similar thermal behavior, and NAAC4 has a higher k if compared with them, although it has a less density.

Theoretically one must expect that with concrete density decrease, there will also be k decrease, and as moisture increases, k increases, but NAAC 3 and NAAC4 show k values with different trend (Table 3). In dry state, both have similar k (0.71 W/m.K), and values close to k of NAAC1 (0.72 W/m.K). Although NAAC4 has a lower absorption than NAAC3 (Table 2) it presents a higher thermal conductivity with higher moisture (Fig. 3), supposedly related to the characteristics of the bubbles or its distribution.

Table 2 Density (ρ), bulk density (γ), absorption after immersion (%), volume of permeable voids (%), compressive strength (f_c), efficiency factor (EF).

Type of concrete	ρ (kg/m ³)	γ (kg/m ³)	Absorption after immersion (%)	Volume of voids (%)	f_c (MPa)	EF (MPa.dm ³ /kg)
REF	2,300	2,277	5.8	13.4	61.2	27
NAAC1	2,040	1,995 (-12.4%)	6.4 (+10.3%)	13.1	33.4 (-45.4%)	17
NAAC3	1,880	1,868 (-18.0%)	7.6 (+31.0%)	14.4	18.7 (-69.4%)	10
NAAC4	1,820	1,779 (-21.9%)	7.2 (+24.1%)	13.1	12.1 (-80.2%)	7

Table 3 Thermal conductivity of concretes (with the percentage of increase in brackets) in the several moisture ranges.

Degree of moisture	Thermal conductivity k (W/m.K)			
	REF	NAAC1	NAAC3	NAAC4
Dry	1.36	0.72	0.71	0.71
0%-2%	1.52 (+11.8%)	0.82 (+13.9%)	0.75 (+5.6%)	1.00 (+40.8%)
2%-4%	1.59 (+16.9%)	0.84 (+18.3%)	0.88 (+23.9%)	1.02 (+43.7%)
4%-6%	1.76 (+29.4%)	0.96 (+33.3%)	0.92 (+29.6%)	1.13 (+59.1%)

Air-entrained Concrete: Relationship between Thermal Conductivity and Pore Distribution Analyzed by X-Ray Tomography

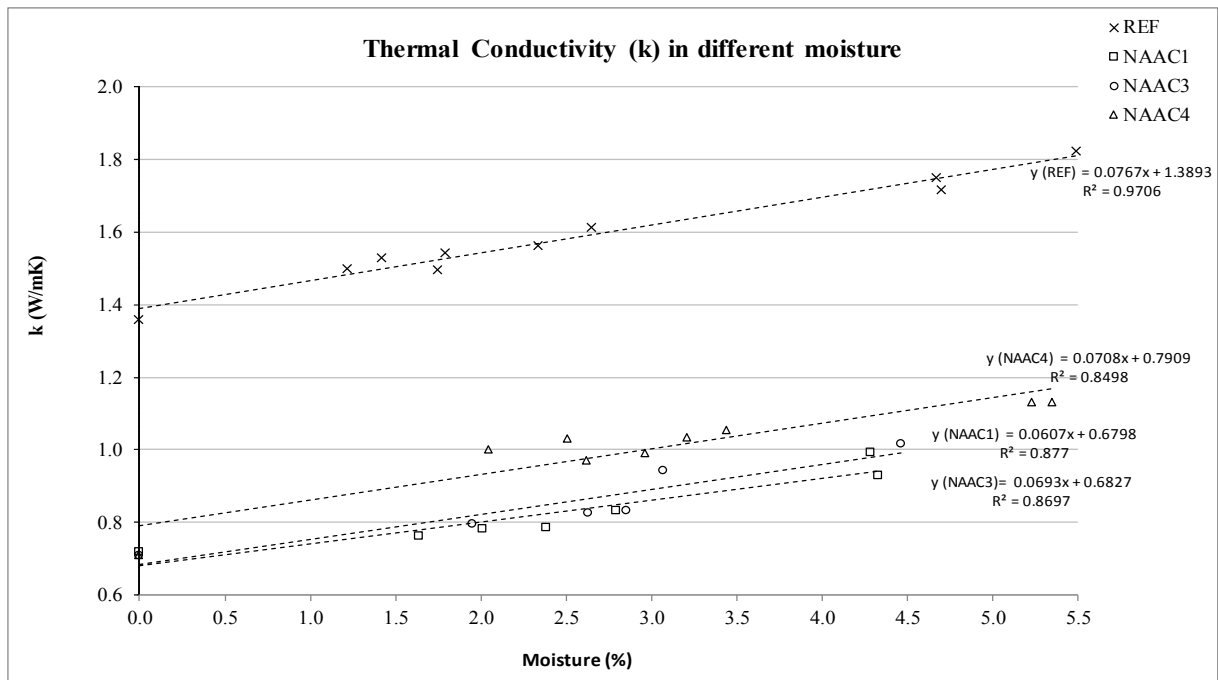


Fig. 3 Thermal conductivity (k) and moisture content (%) of samples.

3.3 Microstructure Analysis by μ CT

Searching to understand the possible causes for the different behavior between NAAC3 and NAAC4 related to “absorption after immersion”, “% of empty spaces” and “k values” (Tables 2 and 3) the microstructure of these samples and sample REF were studied for comparison.

Fig. 4 shows the images of samples REF, NAAC3 and NAAC4 obtained by μ CT in position XY, YZ and XZ in level 630/1004 where some bubbles are highlighted with its diameter.

Images of samples in direction XY in three different levels obtained from by μ CT, are shown in Fig. 5.

After processing the images with the software AVIZO 8.0, the air bubbles in each cylindrical specimen were quantified. It was counted 9,691 bubbles for sample REF: 40,854 for sample NAAC3; and 38,851 for NAAC4. Fig. 6 shows the volume distribution of bubbles for samples REF, NAAC3 and NAAC4.

Concerning the volume of bubbles (Fig. 6), REF and NAAC4 had the larger volume formed by bubbles $>500 \mu\text{m}$, which was considered as “occasionally entrapped” or “from coalescence”, with

$6.1 \times 10^{10} \mu\text{m}^3$ (71%) and $8.13 \times 10^{10} \mu\text{m}^3$ (57%) respectively, and NAAC3 has the volume better distributed in bubbles with smaller pores and higher number of bubbles with diameter ranging between 100-150 μm . Fig. 7 shows the bubble diameter count distribution in various size ranges.

Analyzing the distribution of the number of bubbles (Fig. 7) NAAC3 has a larger amount of bubbles smaller than 100 μm (31,903 or 78%), while NAAC4 has 25,946 of bubbles with these characteristics representing 66%.

This characteristic (Figs. 6 and 7) can be the elucidation of the same thermal conductivity of NAAC3 and NAAC4 in dry state ($k = 0.71 \text{ W/m.K}$) even NAAC3 having a greater density if compared NAAC4 ($1,868 \text{ kg/m}^3$ and $1,779 \text{ kg/m}^3$) respectively. The bubble distribution also explains the fact that the thermal conductivity in NAAC4 is more susceptible to moisture comparing to NAAC3, while k of NAAC3 has an increase of 29.6% (compared with dry state) in moisture ranging between 4% and 6%, NAAC4 has an increase of 59.1% in same condition, though absorption after immersion of NAAC4 is less than NAAC3, 7.2% and 7.6% receptivity (Table 3).

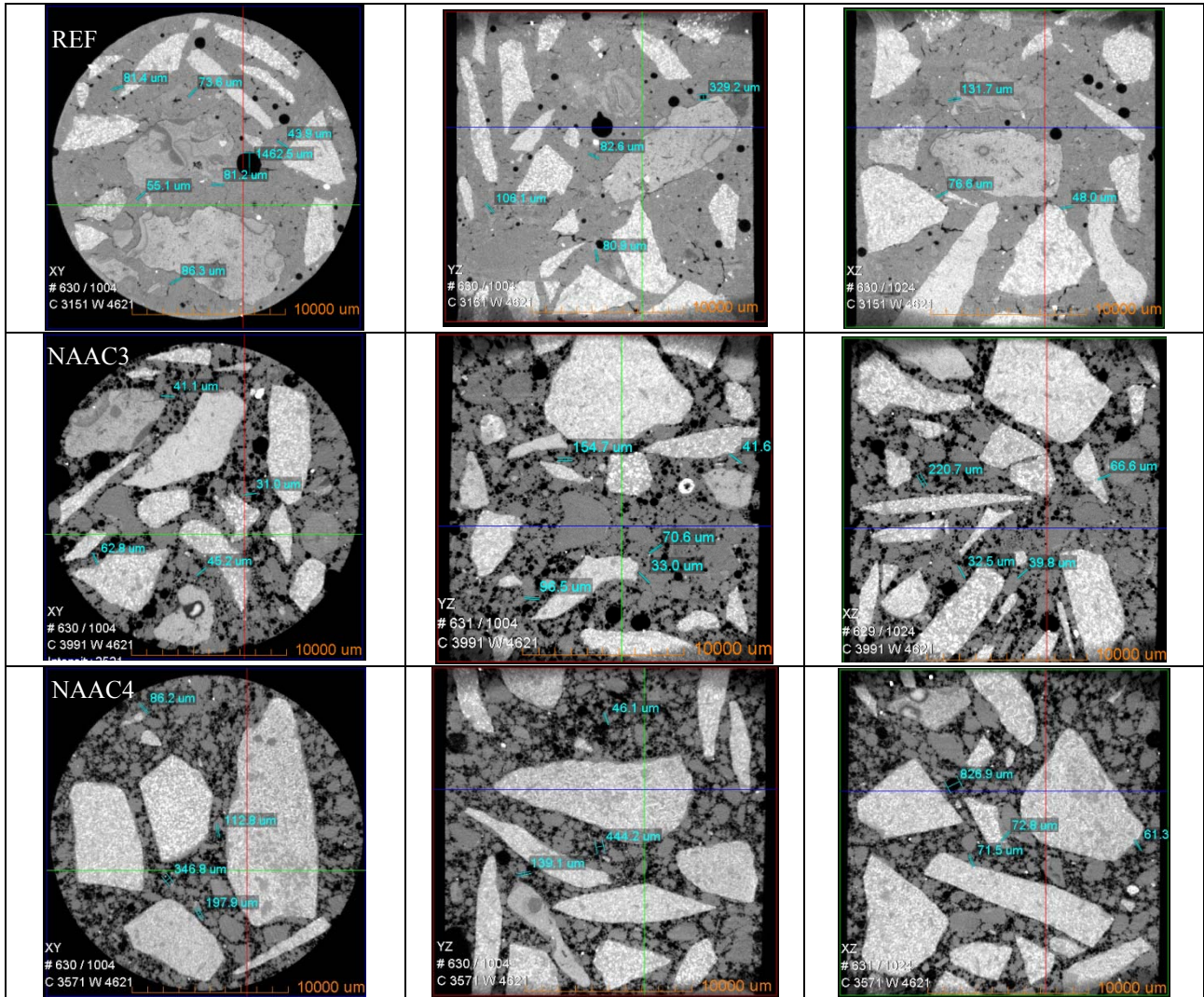


Fig. 4 Images of samples REF, NAAC3, NAAC4 in directions XY, YZ and XZ obtained by μCT.

Air-entrained Concrete: Relationship between Thermal Conductivity and Pore Distribution Analyzed by X-Ray Tomography

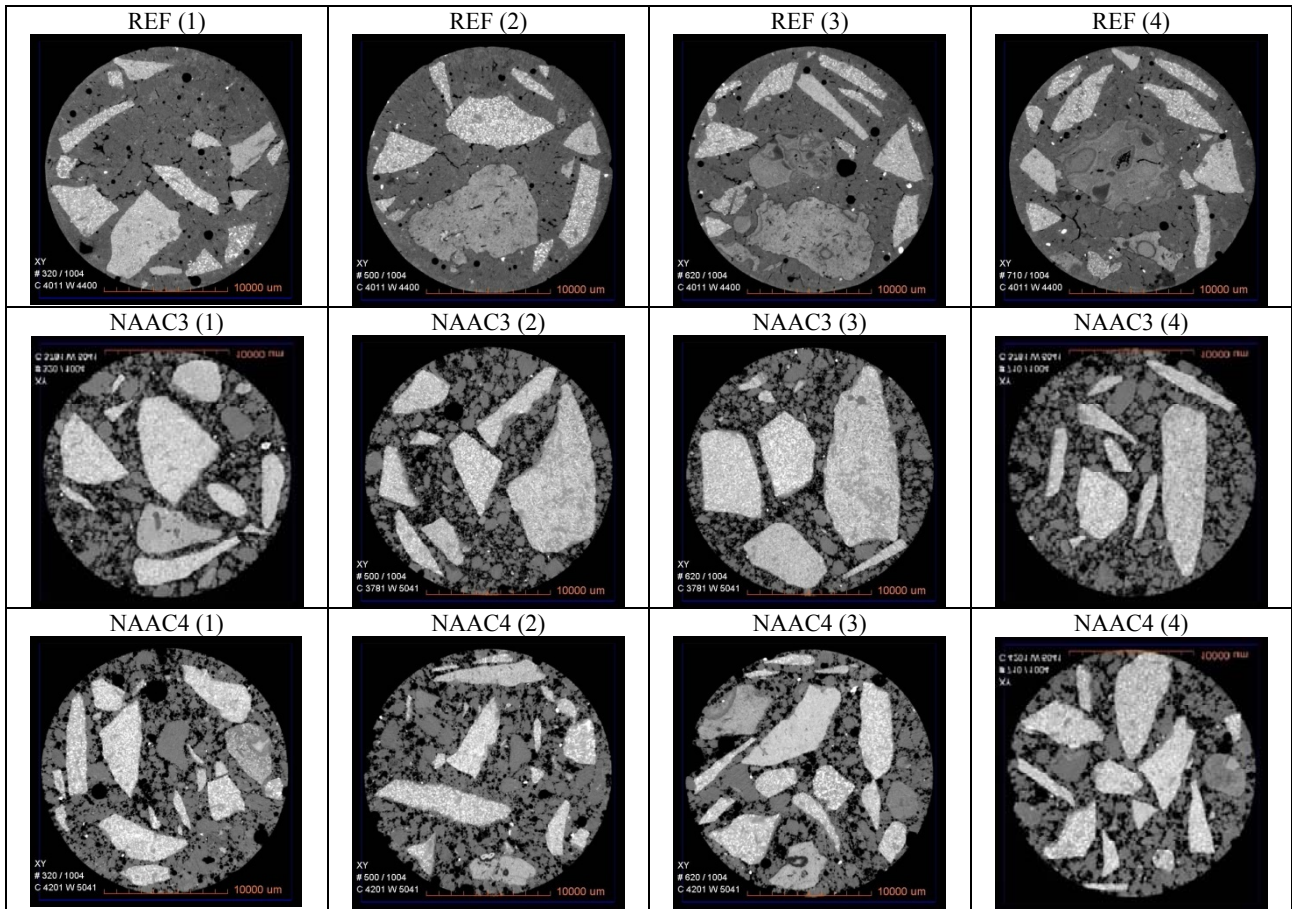


Fig. 5 Images of samples REF, NAAC3, NAAC4 in the direction of XY in three additional levels obtained by μCT.

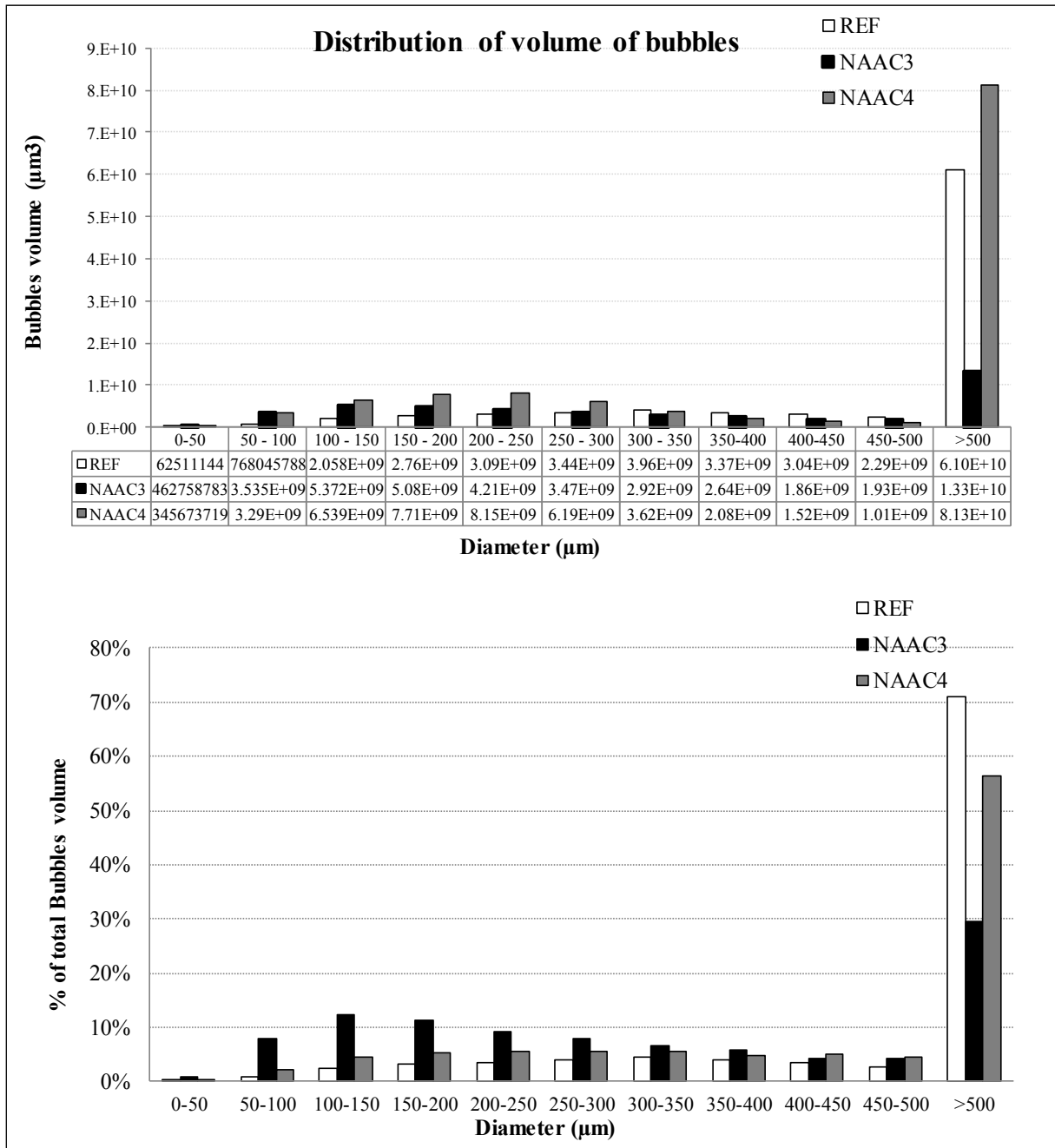


Fig. 6 Bubble volume distribution (%) by μCT images of cylindrical specimens.

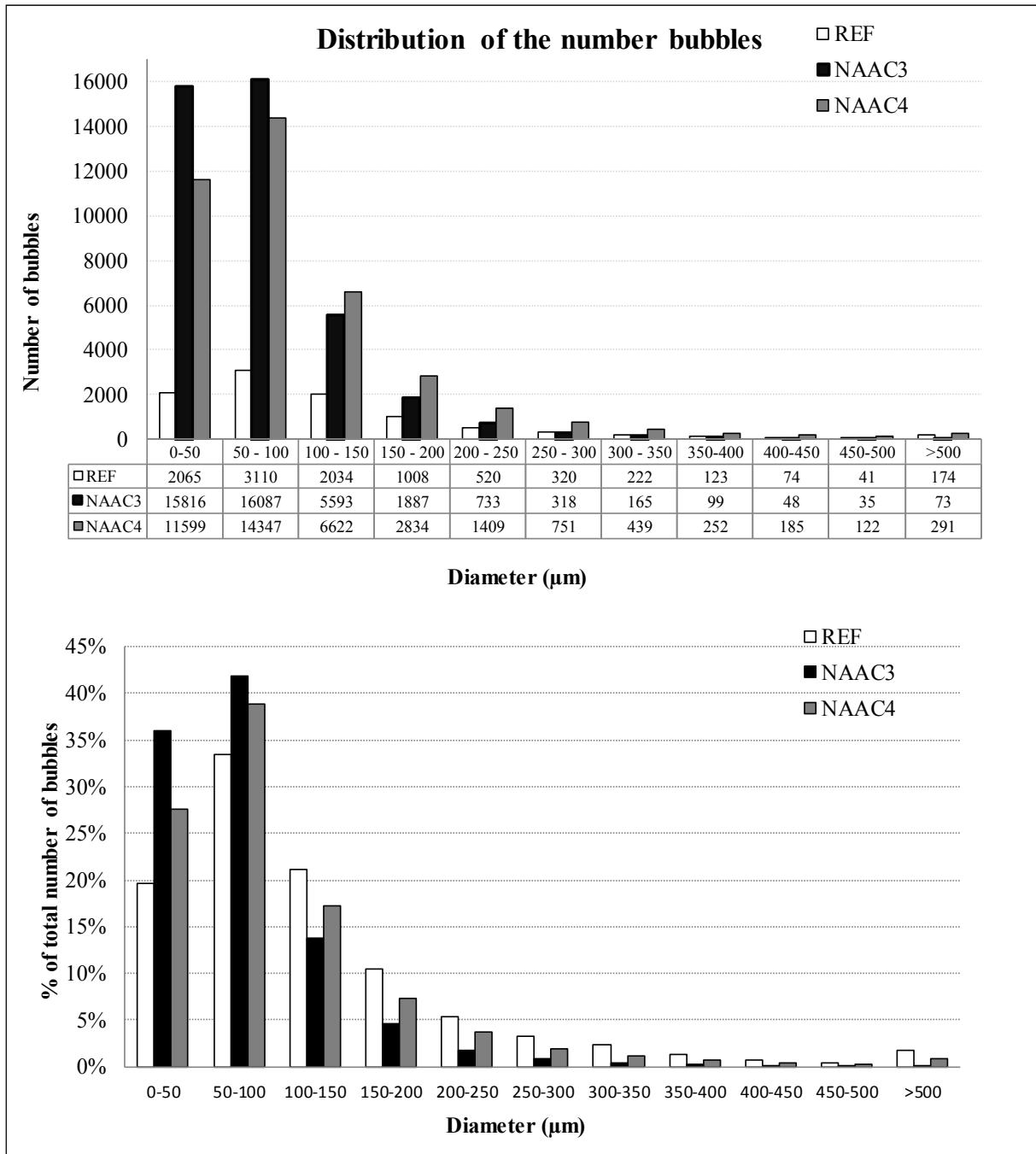


Fig. 7 Number of bubbles in the size ranges determined by μ CT images of cylindrical specimens.

4. Conclusions

The results of the thermal conductivity in this study, in dry or wet state, show that air-entrainment leads to viable use of this material as sealer to achieve good thermal insulation, and it can be adjusted up to get the appropriate k value so the concrete can be used in walls

as sealing (k about 0.8 W/m.K is recommended). On the other hand, the decrease of its density to values below 2,000 kg/m³ does not mean lower k values which justify worse mechanical performance or a greater susceptibility of the structure regarding durability.

The k values in wet state show that the bubble

distribution has meaningful influence in the susceptibility of the concrete k related to moisture: a larger amount of bubbles with smaller diameter represents minor thermal conductivity. In addition, there seems to be a limit to air entraining and, if it is exceeded the bubbles starts to coalesce (such as NAAC4), leading to bigger thermal conductivity, lower density and worse mechanical performance.

The analysis of images obtained by μ CT has been shown to be a valuable resource for the correct understanding of the influence of the bubble distribution on the performance of air-entrained concrete. However further studies are required to verify the bubbles connectivity, mainly by simulating the flow of a fluid (e.g. air) through the concrete.

Acknowledgement

This work was carried out with the collaboration of the FECIV-UFU, Construction Laboratory of IAUSC-USP, Geotechnical Department of the EESC-USP; LCT-EPUSP fellow researchers Daniel Uliana and Fabrizzio Costa; and FZEA-USP mainly Prof. Dr. Holmer Savastano Junior. We would like to express our gratitude to them.

References

- [1] Budaiwi, I., Abdou, A., and Al-Hormoud. 2002. "Variations of Thermal Conductivity of Insulation Materials under Different Operating Temperatures: Impact on Envelope-Induce Cooling Load." *J. Archit. Eng.* 10 (1061): 125-32.
- [2] Bazant, Z. P., and Kaplan, M. F. 1996. *Concrete at Temperatures, Material Properties and Mathematical Models*. Essex, UK: Logman.
- [3] Holm, T. A., and Bremner, T. W. 2000. *State-of-Art Report on High-Strength, High-Durability Structural Low-Density Concrete for Applications in Severe Marine Environments*. Washington, DC, USA: US Army Engineer Research and Development Center.
- [4] Wei, S., Yunsheng, Z., and Jones, M. R. 2014. "Three-Dimensional Numerical Modeling and Simulation of the Thermal Properties of Foamed Concrete." *Construction and Building Materials* 50: 421-31.
- [5] Bhattacharjee, B., and Krishnamoorthy, S. 2004. "Permeable Porosity and Thermal Conductivity of Construction Materials." *J. Mat. Civil. Eng.* 10 (1061): 322-30.
- [6] Narayanan, N., and Ramamurthy, K. 2000. "Structure and Properties of Aerated Concrete: A Review." *Cement & Concrete Composites* 22: 321-9.
- [7] Neville, A. M. 2016. *Propriedades do concreto*. Porto Alegre, Brazil: Bookman.
- [8] Piekarczyk, B. L. 2013. "The Type of Air-Entraining and Viscosity Modifying Admixtures and Porosity and Frost Durability of High Performance Self-compacting Concrete." *Construction and Building Materials* 40: 659-71.
- [9] Moravcová, B., Possl, P., Misák, P., and Michal Blazek, M. 2016. "Possibilities of Determining the Air-Pore Content in Cement Composites Using Computed Tomography and Other Methods." *Materials and Technology* 50 (4): 491-8.
- [10] Hilal, A. A., Thom, N. H., and Dawson, A. R. 2015. "On Entrained Pore Size Distribution of Foamed Concrete." *Construction and Building Materials* 75: 227-33.
- [11] Lu, H., Alymov, E., Shah, S., and Peterson, K. 2017. "Measurement of Air Void System in Lightweight Concrete by X-Ray Computed Tomography." *Construction and Building Materials* 152: 467-83.
- [12] ACI 122R-02. 2002. "Guide to Thermal Properties of Concrete and Masonry Systems." In *ACI Manual of Concrete Practise*, Chapter 122R-02. American Concrete Institute, Detroit.
- [13] Goual, M. S., Bali, A., and Quéneudec, M. 1999. "Effective Thermal Conductivity of Clayey Aerated Concrete in the Dry State: Experimental Results and Modeling." *J. Phys.* 32 (23): 3041-6.
- [14] ASTM C34-13. 2013. "Standard Specification for Structural Clay Load-Bearing Wall Tile." <https://doi.org/10.1520/C0034>.
- [15] ASTM C642-13. 2013. "Standard Test Method for Density, Absorption, and Voids in Hardened Concrete." <https://doi.org/10.1520/C0642-13>.
- [16] ASTM E1530-11. 2011. "Standard Test Method for Evaluating the Resistance to Thermal Transmission of Materials by the Guarded Heat Flow Meter Technique." <https://doi.org/10.1520/E1530-11>.
- [17] Kodur, V., and Khaliq, W. 2011. "Effect of Temperature on Thermal Properties of Different Types of High-Strength Concrete." *J. Mat. Civil. Eng.* 10 (1061): 793-801.